



UNIVERSITÀ
DEGLI STUDI
FIRENZE

FLORE

Repository istituzionale dell'Università degli Studi di Firenze

Phase transitions in Thirring's model

Questa è la Versione finale referata (Post print/Accepted manuscript) della seguente pubblicazione:

Original Citation:

Phase transitions in Thirring's model / Campa, Alessandro; Casetti, Lapo; Latella, Ivan; Pérez-Madrid, Agustín; Ruffo, Stefano. - In: JOURNAL OF STATISTICAL MECHANICS: THEORY AND EXPERIMENT. - ISSN 1742-5468. - ELETTRONICO. - 2016:(2016), pp. 073205-073205. [10.1088/1742-5468/2016/07/073205]

Availability:

The webpage <https://hdl.handle.net/2158/1080523> of the repository was last updated on 2017-05-05T16:58:52Z

Published version:

DOI: 10.1088/1742-5468/2016/07/073205

Terms of use:

Open Access

La pubblicazione è resa disponibile sotto le norme e i termini della licenza di deposito, secondo quanto stabilito dalla Policy per l'accesso aperto dell'Università degli Studi di Firenze (<https://www.sba.unifi.it/upload/policy-oa-2016-1.pdf>)

Publisher copyright claim:

La data sopra indicata si riferisce all'ultimo aggiornamento della scheda del Repository FloRe - The above-mentioned date refers to the last update of the record in the Institutional Repository FloRe

(Article begins on next page)

Phase transitions in Thirring's model

Alessandro Campa¹, Lapo Casetti^{2,3}, Ivan Latella⁴, Agustín Pérez-Madrid⁴ and Stefano Ruffo^{2,5}

¹ Complex Systems and Theoretical Physics Unit, Health and Technology Department, Istituto Superiore di Sanità, and INFN Roma 1, Gruppo Collegato Sanità, Viale Regina Elena 299, 00161 Roma, Italy

² Dipartimento di Fisica e Astronomia and CSDC, Università di Firenze, and INFN, Sezione di Firenze, via G. Sansone 1, 50019 Sesto Fiorentino (FI), Italy

³ INAF-Osservatorio Astrofisico di Arcetri, Largo E. Fermi 5, 50125 Firenze, Italy

⁴ Departament de Física de la Matèria Condensada, Facultat de Física, Universitat de Barcelona, Martí i Franquès 1, 08028 Barcelona, Spain

⁵ SISSA, via Bonomea 265, CNISM and INFN, 34136 Trieste, Italy

E-mail: alessandro.campa@iss.infn.it, lapo.casetti@unifi.it, ilatella@ffn.ub.edu, agustiperezmadrid@ub.edu and ruffo@sissa.it

Abstract. In his pioneering work on negative specific heat, Walter Thirring introduced a model that is solvable in the microcanonical ensemble. Here, we give a complete description of the phase-diagram of this model in both the microcanonical and the canonical ensemble, highlighting the main features of ensemble inequivalence. In both ensembles, we find a line of first-order phase transitions which ends in a critical point. However, neither the line nor the point have the same location in the phase-diagram of the two ensembles. We also show that the microcanonical and canonical critical points can be analytically related to each other using a Landau expansion of entropy and free energy, respectively, in analogy with what has been done in [O. Cohen, D. Mukamel, J. Stat. Mech., P12017 (2012)]. Examples of systems with certain symmetries restricting the Landau expansion have been considered in this reference, while no such restrictions are present in Thirring's model. This leads to a phase diagram that can be seen as a prototype for what happens in systems of particles with kinematic degrees of freedom dominated by long-range interactions.

1. Introduction

In recent years, the systematic study of systems with long-range interactions has attracted considerable attention, due to remarkable properties that significantly differ from those of short-range interacting systems [1–4]. Examples of such systems are self-gravitating systems [5–13], plasmas [14, 15], two-dimensional and geophysical fluids [16–20] and spin systems [21, 22]. The long-range character of the interactions confers a striking property to these systems: they are intrinsically non additive. Non additivity, however, does not hinder neither a statistical mechanical formulation [1] nor a proper thermodynamic description [23]. Because of non additivity, equilibrium configurations may present negative specific heat in the microcanonical ensemble [6, 8], ensemble inequivalence [8, 24–26] and the violation of the usual Gibbs-Duhem equation [23, 27]. A feature which is of direct relevance for this paper is that non additivity, which is responsible for changes in the concavity of the thermodynamic potentials, directly leads to ensemble inequivalence. This latter is in turn manifest through the properties of the phase-diagrams, which are not the same in different ensembles.

A seminal work on negative specific heat was written by Walter Thirring [8]. In that paper he introduced a simple model that reproduces some of the properties of self-gravitating systems. He showed that the model exhibits negative specific heat and temperature jumps in the microcanonical ensemble and that they are both absent, and replaced by a first-order phase transition, in the canonical ensemble. In the last decade, ensemble inequivalence in non additive systems has become an established fact [1], and several different models have been shown to display such a feature.

However, quite surprisingly, a detailed study of the full phase diagram in both the microcanonical and the canonical ensemble of Thirring's model has not yet been performed. Moreover, the analysis of ensemble inequivalence has been restricted in general to models which are endowed with specific symmetries of the order parameter. We are here thinking, for instance, to models of magnetic systems which, in absence of an external field, are invariant under a sign change $m \rightarrow -m$ of magnetization m . These models have typically a phase diagram with a line of second order phase transitions which ends at a tricritical point. This latter has a different location in different ensembles [25]. Thirring's model does not possess this symmetry and, as we will show, the line of first-order phase transitions terminates at a critical point, as it happens for the gas-liquid phase transitions in fluids. At variance with what is found for models with symmetries, ensemble inequivalence manifests itself in Thirring's model by a different location of the critical point. In addition, the mean-field character of Thirring's model allows us to employ a Landau expansion [28] of thermodynamic potentials and to determine analytically the location of the critical point in both the microcanonical and canonical ensembles.

Using a Landau expansion for the thermodynamic potentials, phase diagrams and ensemble inequivalence in systems with two types of symmetry have been considered in [29]. There, these symmetries are specified by $f(m, q) = f(-m, q)$ and $f(m, q) =$

$f(-m, -q)$, where m is the order parameter and f is the thermodynamic potential corresponding to the “lower” ensemble in which the thermodynamic variable q is fixed, while this variable can fluctuate in the “higher” ensemble. Furthermore, the ABC model [30,31], a one-dimensional driven exclusion model, and the anisotropic XY model for a system with infinite-range interacting spins have been discussed in [29] as concrete examples. These models consist of lattice sites with internal degrees of freedom; on the contrary, Thirring's model is a simplified version of a self-gravitating system, and as such it describes particles with kinematic degrees of freedom. In addition and in contrast to the previous examples, Thirring's model has no symmetries restricting the Landau expansion, leading to a phase diagram that can be seen as a prototype for what happens in systems of particles with kinematic degrees of freedom dominated by long-range interactions.

2. Thirring's model

Thirring's model is a minimal model that describes a confined system with regularized attractive interactions that mimic those of a self-gravitating gas [32,33]. In this model, N particles of mass m are enclosed in a volume V with a Hamiltonian given by

$$\mathcal{H} = \sum_{i=1}^N \frac{|\mathbf{p}_i|^2}{2m} + \sum_{i>j}^N \phi(\mathbf{q}_i, \mathbf{q}_j), \quad (1)$$

where \mathbf{p}_i is the momentum of the i -th particle, and the interactions are defined by the nonlocal potential [8]

$$\phi(\mathbf{q}_i, \mathbf{q}_j) = -2\nu\theta_{V_0}(\mathbf{q}_i)\theta_{V_0}(\mathbf{q}_j). \quad (2)$$

Here $\nu > 0$ is a constant, and $\theta_{V_0}(\mathbf{q}_i) = 1$ if $\mathbf{q}_i \in V_0$ and vanishes otherwise, where \mathbf{q}_i is the position of the i -th particle and $V_0 < V$ is the core volume. Particles outside V_0 are free, so that the total potential energy in the large N limit is given by

$$\sum_{i>j}^N \phi(\mathbf{q}_i, \mathbf{q}_j) = -\nu N_0^2, \quad (3)$$

where N_0 is the number of particles in V_0 for a given configuration. Notice that, as a consequence of the interaction potential (2), the system is nonadditive [23] and exhibits the rich phenomenology common to long-range interacting systems. In particular, the microcanonical and canonical ensembles are not equivalent, as will be shown below.

Let us consider the thermodynamics of the system when it is isolated. The density of states in phase space can be written as a sum over all possible values of the number of particles in the core [8]

$$\omega(E, V, N) = \sum_{N_0} e^{\hat{S}(E, V, N, N_0)}, \quad (4)$$

in such a way that the maximization of $\hat{S}(E, V, N, N_0)$ leads to the microcanonical entropy in the large N limit, $S(E, V, N) = \sup_{N_0} \hat{S}(E, V, N, N_0)$. Here and below we

use units in which $k_B = 1$. Furthermore, introducing the fraction of free particles n_g (fraction of particles outside V_0), the reduced energy ε , and the reduced volume η , given by

$$n_g = 1 - \frac{N_0}{N}, \quad \varepsilon = \frac{E}{\nu N^2} + 1, \quad \eta = \ln \left(\frac{V - V_0}{V_0} \right), \quad (5)$$

the function \hat{S} in (4) can be written as $\hat{S} \equiv N\hat{s}$ with [8, 33]

$$\hat{s}(n_g, \varepsilon, \eta) = \frac{3}{2} \ln [\varepsilon - 2n_g + n_g^2] - (1 - n_g) \ln(1 - n_g) - n_g \ln n_g + n_g \eta, \quad (6)$$

where in (6) we have neglected constant terms. The microcanonical entropy per particle $s = S/N$ is thus given by

$$s(\varepsilon, \eta) = \hat{s}(\bar{n}_g, \varepsilon, \eta) = \sup_{n_g} \hat{s}(n_g, \varepsilon, \eta), \quad (7)$$

where $\bar{n}_g = \bar{n}_g(\varepsilon, \eta)$ is the value of n_g that maximizes (6). The energy E , being the sum of the potential energy (3) and of the kinetic energy \mathcal{K} , is bounded from below by $-\nu N^2$, therefore for the reduced energy we have $\varepsilon \geq 0$. Furthermore, for a given reduced energy in the range $0 \leq \varepsilon < 1$, the fraction of free particles n_g is bounded from above by $1 - \sqrt{1 - \varepsilon}$, due to the fact that $\mathcal{K} \geq 0$. On the other hand, for $\varepsilon \geq 1$ the fraction n_g can take any value in the range $0 \leq n_g \leq 1$. In turn, this guarantees that the argument of the logarithm in equation (6) is never negative. The reduced temperature $\tau = T/(\nu N)$, where T is the temperature, takes the form

$$\frac{1}{\tau(\varepsilon, \eta)} = \left. \frac{\partial}{\partial \varepsilon} \hat{s}(n_g, \varepsilon, \eta) \right|_{n_g = \bar{n}_g} = \frac{3}{2} (\varepsilon - 2\bar{n}_g + \bar{n}_g^2)^{-1}, \quad (8)$$

which is guaranteed to be positive from the same observation made above.

In the canonical ensemble, the system is assumed to be in contact with a thermostat, in such a way that the reduced temperature τ is fixed and the energy fluctuates. The reduced canonical free energy is $\varphi = F/(NT)$, F being the canonical free energy. It can be obtained from the microcanonical entropy by computing its Legendre-Fenchel transform [1], namely,

$$\varphi(\tau, \eta) = \inf_{\varepsilon} \left[\frac{\varepsilon}{\tau} - s(\varepsilon, \eta) \right]. \quad (9)$$

The reduced free energy can also be written as

$$\varphi(\tau, \eta) = \hat{\varphi}(\bar{n}_g, \tau, \eta) = \inf_{n_g} \hat{\varphi}(n_g, \tau, \eta), \quad (10)$$

where

$$\hat{\varphi}(n_g, \tau, \eta) = \inf_{\varepsilon} \left[\frac{\varepsilon}{\tau} - \hat{s}(n_g, \varepsilon, \eta) \right], \quad (11)$$

and now the fraction of free particles that minimizes the free energy is a function of the temperature, $\bar{n}_g = \bar{n}_g(\tau, \eta)$. In this case, using (6), the expression (11) can be computed to give

$$\hat{\varphi}(n_g, \tau, \eta) = -\frac{3}{2} \ln \left(\frac{3\tau}{2} \right) + \frac{2n_g - n_g^2}{\tau} + (1 - n_g) \ln(1 - n_g) + n_g \ln n_g - n_g \eta + \frac{3}{2}. \quad (12)$$

Obviously, the constant terms neglected in the entropy (6) are not included. The mean value $\bar{\varepsilon}$ of the reduced energy in the canonical ensemble is given by

$$\bar{\varepsilon}(\tau, \eta) = -\tau^2 \frac{\partial}{\partial \tau} \hat{\varphi}(n_g, \tau, \eta) \Big|_{n_g = \bar{n}_g} = \frac{3\tau}{2} + 2\bar{n}_g - \bar{n}_g^2. \quad (13)$$

An interesting feature of the system is that it undergoes first-order phase transitions in both the microcanonical and canonical ensembles. Using the Landau theory of phase transitions, below we study the critical points in the two ensembles and show explicitly that they differ from each other.

3. Landau theory: Microcanonical ensemble

Let us introduce the deviation $m = n_g - \bar{n}_g$ of the fraction of free particles n_g with respect to a certain reference value \bar{n}_g . This reference value will be the one maximizing equation (6), i.e., the equilibrium value. Thus, we perform a Landau expansion of the entropy (6) in powers of m around \bar{n}_g ,

$$\hat{s}(m, \varepsilon, \eta) = a_s(\bar{n}_g, \varepsilon, \eta) + b_s(\bar{n}_g, \varepsilon, \eta)m + c_s(\bar{n}_g, \varepsilon, \eta)m^2 + d_s(\bar{n}_g, \varepsilon, \eta)m^3 + e_s(\bar{n}_g, \varepsilon, \eta)m^4 + \mathcal{O}(m^5), \quad (14)$$

where the coefficients are given by

$$a_s(\bar{n}_g, \varepsilon, \eta) = \frac{3}{2} \ln(\varepsilon - 2\bar{n}_g + \bar{n}_g^2) - (1 - \bar{n}_g) \ln(1 - \bar{n}_g) - \bar{n}_g \ln \bar{n}_g + \bar{n}_g \eta, \quad (15)$$

$$b_s(\bar{n}_g, \varepsilon, \eta) = \ln\left(\frac{1 - \bar{n}_g}{\bar{n}_g}\right) - \frac{3(1 - \bar{n}_g)}{\varepsilon - 2\bar{n}_g + \bar{n}_g^2} + \eta, \quad (16)$$

$$c_s(\bar{n}_g, \varepsilon, \eta) = \frac{P_\varepsilon(\bar{n}_g)}{2(1 - \bar{n}_g)\bar{n}_g(\varepsilon - 2\bar{n}_g + \bar{n}_g^2)^2}, \quad (17)$$

$$d_s(\bar{n}_g, \varepsilon, \eta) = \frac{1 - 2\bar{n}_g}{6(1 - \bar{n}_g)^2 \bar{n}_g^2} + \frac{3(1 - \bar{n}_g)}{(\varepsilon - 2\bar{n}_g + \bar{n}_g^2)^2} - \frac{4(1 - \bar{n}_g)^3}{(\varepsilon - 2\bar{n}_g + \bar{n}_g^2)^3}, \quad (18)$$

$$e_s(\bar{n}_g, \varepsilon, \eta) = -\frac{\bar{n}_g^3 + (1 - \bar{n}_g)^3}{12(1 - \bar{n}_g)^3 \bar{n}_g^3} - \frac{3}{4(\varepsilon - 2\bar{n}_g + \bar{n}_g^2)^2} - \frac{6(1 - \varepsilon)(1 - \bar{n}_g)^2}{(\varepsilon - 2\bar{n}_g + \bar{n}_g^2)^4}, \quad (19)$$

with

$$P_\varepsilon(\bar{n}_g) \equiv 2\bar{n}_g^4 - 5\bar{n}_g^3 + (8 - 5\varepsilon)\bar{n}_g^2 + (7\varepsilon - 6)\bar{n}_g - \varepsilon^2. \quad (20)$$

We note that the equilibrium states require the conditions $b_s(\bar{n}_g, \varepsilon, \eta) = 0$, defining $\bar{n}_g = \bar{n}_g(\varepsilon, \eta)$, and $c_s(\bar{n}_g, \varepsilon, \eta) \leq 0$. It is not difficult to see that for $0 \leq \varepsilon \leq 1$ these conditions are satisfied by only one value of \bar{n}_g ; therefore a phase transition can occur only for $\varepsilon > 1$.

3.1. Microcanonical critical point

The microcanonical phase diagram in the (ε, η) plane exhibits a line of first-order phase transition that ends at a critical point specified by the reduced energy and volume ε_{mp}

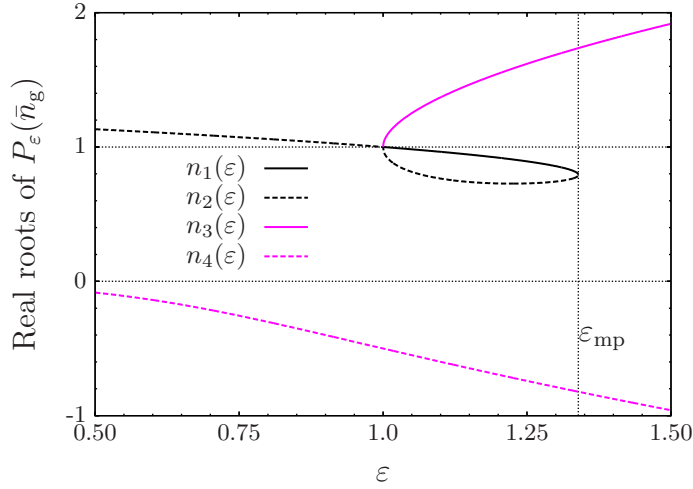


Figure 1. Real roots of $P_\varepsilon(\bar{n}_g)$ as a function of the reduced energy ε . Since, by definition, $0 \leq \bar{n}_g \leq 1$, the roots $n_3(\varepsilon)$ and $n_4(\varepsilon)$ are not to be considered. The roots $n_1(\varepsilon)$ and $n_2(\varepsilon)$ become equal at ε_{mp} , the energy at the microcanonical critical point.

and η_{mp} , respectively, corresponding to a fraction of free particles $\bar{n}_g = n_{\text{mp}}$. Such critical values can be obtained by solving the system of equations

$$\begin{aligned} b_s(n_{\text{mp}}, \varepsilon_{\text{mp}}, \eta_{\text{mp}}) &= 0, \\ c_s(n_{\text{mp}}, \varepsilon_{\text{mp}}, \eta_{\text{mp}}) &= 0, \\ d_s(n_{\text{mp}}, \varepsilon_{\text{mp}}, \eta_{\text{mp}}) &= 0. \end{aligned} \quad (21)$$

In order to find the critical point, consider the quartic polynomial $P_\varepsilon(\bar{n}_g)$ given by (20); when $P_\varepsilon(\bar{n}_g)$ vanishes, also the coefficient c_s vanishes. Let us denote the roots of $P_\varepsilon(\bar{n}_g)$ by $n_i(\varepsilon)$, $i = 1, \dots, 4$. Two of these roots, say, $n_3(\varepsilon)$ and $n_4(\varepsilon)$, lie outside the interval $[0, 1)$ when they are real: since the fraction \bar{n}_g is bounded, $0 \leq \bar{n}_g \leq 1$, these roots are not to be considered. The other two roots, $n_1(\varepsilon)$ and $n_2(\varepsilon)$, can be real or complex, depending on the value of ε , and are given by

$$n_1(\varepsilon) = \frac{\sqrt{3}}{24} \left\{ \frac{15}{\sqrt{3}} + z_2(\varepsilon) - \left[2z_1(\varepsilon) - 18\sqrt{3} \frac{(8\varepsilon + 1)}{z_2(\varepsilon)} \right]^{1/2} \right\}, \quad (22)$$

$$n_2(\varepsilon) = \frac{\sqrt{3}}{24} \left\{ \frac{15}{\sqrt{3}} - z_2(\varepsilon) + \left[2z_1(\varepsilon) + 18\sqrt{3} \frac{(8\varepsilon + 1)}{z_2(\varepsilon)} \right]^{1/2} \right\}, \quad (23)$$

where

$$z_1(\varepsilon) = 16(5\varepsilon - 8) - \frac{4(\varepsilon - 1)(\varepsilon + 26)}{z_3(\varepsilon)} - 4z_3(\varepsilon) + 75, \quad (24)$$

$$z_2(\varepsilon) = \left[80\varepsilon + 8z_3(\varepsilon) + \frac{8(\varepsilon - 1)(\varepsilon + 26)}{z_3(\varepsilon)} - 53 \right]^{1/2}, \quad (25)$$

$$z_3(\varepsilon) = \left[\frac{3\sqrt{3}}{2} \sqrt{-\Delta_P(\varepsilon)} + (1374 - 485\varepsilon)\varepsilon^2 - 1293\varepsilon + 404 \right]^{1/3}, \quad (26)$$

and

$$\Delta_P(\varepsilon) = -36(\varepsilon - 1)^3 (968\varepsilon^3 - 2581\varepsilon^2 + 2276\varepsilon - 744) \quad (27)$$

is the discriminant of $P_\varepsilon(\bar{n}_g)$. When $n_1(\varepsilon)$ and $n_2(\varepsilon)$ are real, they lie in the interval $(0, 1]$ for a certain range of energies ε . To visualize this situation, we plot in figure 1 the real roots of $P_\varepsilon(\bar{n}_g)$ as function of ε . In addition, these roots are real and different when the discriminant is positive, are real and degenerate when $\Delta_P(\varepsilon)$ vanishes, and become complex when $\Delta_P(\varepsilon)$ is negative. Thus, the solution of the system (21) is characterized by the condition $\Delta_P(\varepsilon_{\text{mp}}) = 0$, in such a way that $n_{\text{mp}} = n_1(\varepsilon_{\text{mp}}) = n_2(\varepsilon_{\text{mp}})$. This can be seen by noting that c_s is continuous for \bar{n}_g between n_1 and n_2 , and that

$$d_s(\bar{n}_g, \varepsilon, \eta) = \frac{1}{3} \frac{\partial}{\partial \bar{n}_g} c_s(\bar{n}_g, \varepsilon, \eta), \quad (28)$$

so that the value of \bar{n}_g that cancels out d_s must lie between n_1 and n_2 . Therefore, if the fraction $\bar{n}_g = n_{\text{mp}}$ cancels out both c_s and d_s , we have $n_{\text{mp}} = n_1 = n_2$, which is precisely what happens when the discriminant vanishes, $\Delta_P(\varepsilon_{\text{mp}}) = 0$. Furthermore, in such a case, from $b_s(n_{\text{mp}}, \varepsilon_{\text{mp}}, \eta_{\text{mp}}) = 0$, the critical reduced volume can be unequivocally determined as

$$\eta_{\text{mp}} = \frac{3(1 - n_{\text{mp}})}{\varepsilon_{\text{mp}} - 2n_{\text{mp}} + n_{\text{mp}}^2} - \ln \left(\frac{1 - n_{\text{mp}}}{n_{\text{mp}}} \right). \quad (29)$$

The discriminant $\Delta_P(\varepsilon)$, equation (27), is a polynomial of degree six in ε . It has four real roots and two complex roots: three of these real roots are found at $\varepsilon_0 = 1$, and the remaining real root is given by

$$\varepsilon_{\text{mp}} = \frac{(k_1 + k_2)^{1/3} + (k_1 - k_2)^{1/3} + 2581}{2904} \simeq 1.339, \quad (30)$$

with the numerical coefficients $k_1 = 1016263261$ and $k_2 = 37792656\sqrt{723}$. We note that ε_0 is not the critical energy at the critical point, since one has $n_1(\varepsilon_0) = n_2(\varepsilon_0) = 1$ and, hence, this corresponds, from equation (29), to a state with $\eta \rightarrow \infty$. The critical fraction can be obtained by evaluating equations (22) or (23) at the critical energy ε_{mp} , yielding $n_{\text{mp}} \simeq 0.7929$. Finally, from (29), the critical reduced volume is given by $\eta_{\text{mp}} \simeq 2.969$.

In addition, we note that phase transitions can occur only for ε such that $\varepsilon_0 < \varepsilon < \varepsilon_{\text{mp}}$, since for $\varepsilon < 1$, as noted before, the condition $b_s(\bar{n}_g, \varepsilon, \eta) = 0$ defines only one state of equilibrium. In figure 2 we show the microcanonical phase diagram in the (ε, η) plane, with the line of first order transition points terminating at the critical point. The features of the microcanonical and canonical phase diagrams are commented later.

4. Landau theory: Canonical ensemble

We are interested in showing how the phase diagram in the canonical ensemble differs from the diagram obtained in the microcanonical ensemble. Following [29], we introduce the deviation $q = \varepsilon - \bar{\varepsilon}$ of the energy with respect to the mean value $\bar{\varepsilon}$ and perform an

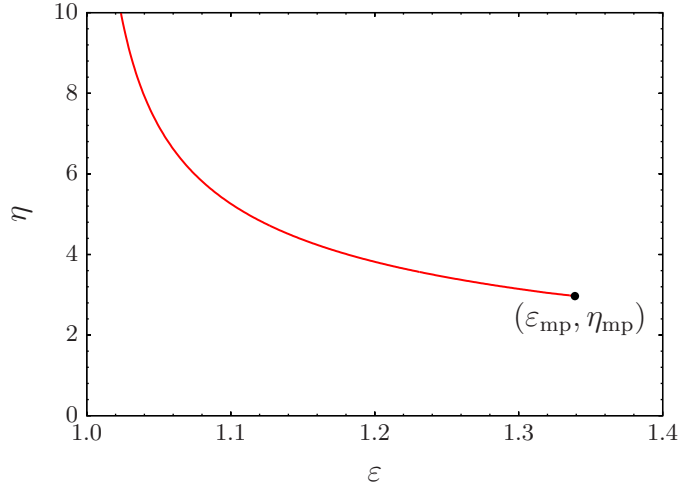


Figure 2. Phase diagram in the (ε, η) plane, showing the transition line in the microcanonical ensemble. The plot shows the curve $\eta(\varepsilon)$, which represents the points defined by the reduced energy ε and reduced volume η at which first-order phase transitions take place in the microcanonical ensemble. The transition line terminates at a critical point represented by the point $(\varepsilon_{\text{mp}}, \eta_{\text{mp}})$. The values of the critical parameters are $\varepsilon_{\text{mp}} \simeq 1.339$ and $\eta_{\text{mp}} \simeq 2.969$.

expansion in powers of q of the entropy in such a way that

$$\frac{\varepsilon}{\tau} - \hat{s}(m, \varepsilon, \eta) = \frac{\bar{\varepsilon} + q}{\tau} - a_0 - a_1 q - a_2 q^2 - a_3 q^3 - (b_0 + b_1 q + b_2 q^2) m - (c_0 + c_1 q) m^2 - d_0 m^3 + \mathcal{O}(m^4) \quad (31)$$

where we have used (14) and the coefficients of the expansion are given by

$$\alpha_k \equiv \frac{1}{k!} \left. \frac{\partial^k}{\partial \varepsilon^k} \alpha_s(\bar{n}_g, \varepsilon, \eta) \right|_{\varepsilon=\bar{\varepsilon}}, \quad \alpha = a, b, c. \quad (32)$$

Fixing the temperature to that of the state at which $\varepsilon = \bar{\varepsilon}$ and $m = 0$, such that

$$\frac{1}{\tau} = \left. \frac{\partial}{\partial \varepsilon} \hat{s}(m, \varepsilon, \eta) \right|_{m=0, \varepsilon=\bar{\varepsilon}} = a_1, \quad (33)$$

and minimizing (31) with respect to q yields

$$q = -\frac{b_1}{2a_2} m - \frac{4a_2^2 c_1 - 4a_2 b_1 b_2 + 3a_3 b_1^2}{8a_2^3} m^2 + \mathcal{O}(m^3), \quad (34)$$

as well as a second solution given by

$$q_2 = -\frac{2a_2}{3a_3} - \frac{2b_2}{3a_3} m - q. \quad (35)$$

We do not consider the solution q_2 because it does not vanish at $m = 0$. Therefore, using equations (33) and (34) in (31) and replacing the latter in (11) gives

$$\begin{aligned} \hat{\varphi}(m, \tau, \eta) = & \frac{\bar{\varepsilon}}{\tau} - a_0 - b_0 m + \left(\frac{b_1^2}{4a_2} - c_0 \right) m^2 \\ & + \left(\frac{4a_2^2 b_1 c_1 - 2a_2 b_1^2 b_2 + a_3 b_1^3}{8a_2^3} - d_0 \right) m^3 + \mathcal{O}(m^4). \end{aligned} \quad (36)$$

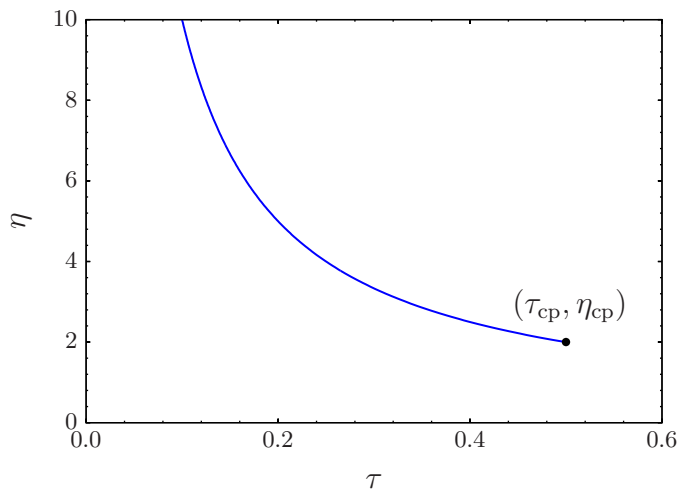


Figure 3. Phase diagram in the (τ, η) plane, showing the transition line in the canonical ensemble. The plot shows the curve $\eta(\tau)$, which represents the points defined by the reduced temperature τ and reduced volume η at which first-order phase transitions take place in the canonical ensemble. The transition line terminates at a critical point represented by the point $(\tau_{\text{cp}}, \eta_{\text{cp}})$. The values of the critical parameters are $\tau_{\text{cp}} = 1/2$ and $\eta_{\text{cp}} = 2$.

By writing the free energy as

$$\hat{\varphi}(m, \tau, \eta) = a_{\varphi}(\bar{n}_{\text{g}}, \tau, \eta) + b_{\varphi}(\bar{n}_{\text{g}}, \tau, \eta)m + c_{\varphi}(\bar{n}_{\text{g}}, \tau, \eta)m^2 + d_{\varphi}(\bar{n}_{\text{g}}, \tau, \eta)m^3 + e_{\varphi}(\bar{n}_{\text{g}}, \tau, \eta)m^4 + \mathcal{O}(m^5), \quad (37)$$

one identifies the coefficients

$$a_{\varphi}(\bar{n}_{\text{g}}, \tau, \eta) = \frac{\bar{\varepsilon}}{\tau} - a_0, \quad (38)$$

$$b_{\varphi}(\bar{n}_{\text{g}}, \tau, \eta) = -b_0, \quad (39)$$

$$c_{\varphi}(\bar{n}_{\text{g}}, \tau, \eta) = \frac{b_1^2}{4a_2} - c_0, \quad (40)$$

$$d_{\varphi}(\bar{n}_{\text{g}}, \tau, \eta) = \frac{4a_2^2 b_1 c_1 - 2a_2 b_1^2 b_2 + a_3 b_1^3}{8a_2^3} - d_0, \quad (41)$$

where the mean energy $\bar{\varepsilon}$ must be taken as a function of τ whose dependence is obtained through (33). Since $\hat{s}(m, \bar{\varepsilon}, \eta) = a_0 + b_0 m + c_0 m^2 + d_0 m^3 + \mathcal{O}(m^4)$, the previous procedure provides the first terms of the Landau expansion of the canonical free energy as functions of the coefficients of the expansion of the microcanonical entropy at a certain energy $\varepsilon = \bar{\varepsilon}$. We observe that the coefficients c_{φ} and d_{φ} do not vanish at the same critical conditions that c_0 and d_0 do. Hence, the critical point in the canonical ensemble will be different from the corresponding one in the microcanonical ensemble.

We highlight that we have started from a generic Landau expansion of the entropy. For Thirring's model $\bar{\varepsilon}$ is given by (13) and the coefficients in the microcanonical ensemble by equations (15)-(19), so that using equations (39), (40), and (41) one obtains

$$b_{\varphi}(\bar{n}_{\text{g}}, \tau, \eta) = \frac{2(1 - \bar{n}_{\text{g}})}{\tau} - \ln \left(\frac{1 - \bar{n}_{\text{g}}}{\bar{n}_{\text{g}}} \right) - \eta, \quad (42)$$

$$c_\varphi(\bar{n}_g, \tau, \eta) = \frac{Q_\tau(\bar{n}_g)}{\tau(1-\bar{n}_g)\bar{n}_g}, \quad (43)$$

$$d_\varphi(\bar{n}_g, \tau, \eta) = \frac{1}{6} \left[-\frac{1}{\bar{n}_g^2} + \frac{1}{(1-\bar{n}_g)^2} \right], \quad (44)$$

with

$$Q_\tau(\bar{n}_g) \equiv \bar{n}_g^2 - \bar{n}_g + \frac{\tau}{2}. \quad (45)$$

The equilibrium states in the canonical ensemble require the conditions $b_\varphi(\bar{n}_g, \tau, \eta) = 0$, defining $\bar{n}_g = \bar{n}_g(\tau, \eta)$, and $c_\varphi(\bar{n}_g, \tau, \eta) \geq 0$.

4.1. Canonical critical point

As it happens in the microcanonical ensemble in the (ε, η) plane, the canonical phase diagram exhibits in the (τ, η) plane a line of first-order phase transition that ends at a critical point, here specified by the reduced temperature and volume τ_{cp} and η_{cp} , respectively, for which the fraction of free particles is denoted by n_{cp} . The critical parameters can now be obtained by solving the system of equations

$$\begin{aligned} b_\varphi(n_{\text{cp}}, \tau_{\text{cp}}, \eta_{\text{cp}}) &= 0, \\ c_\varphi(n_{\text{cp}}, \tau_{\text{cp}}, \eta_{\text{cp}}) &= 0, \\ d_\varphi(n_{\text{cp}}, \tau_{\text{cp}}, \eta_{\text{cp}}) &= 0. \end{aligned} \quad (46)$$

Since d_φ depends only on \bar{n}_g , one immediately obtains that the critical point can occur only for $n_{\text{cp}} = \bar{n}_g = 1/2$. Substituting it in equation (43) or equation (45) one then finds that the critical temperature is $\tau_{\text{cp}} = 1/2$. Finally, replacing these values in equation (42) we get that $\eta_{\text{cp}} = 2$. However, it is useful to consider the discriminant of the quadratic polynomial $Q_\tau(\bar{n}_g)$, given in equation (45), following a procedure analogous to that used in the microcanonical case, where the discriminant of the quartic polynomial $P_\varepsilon(\bar{n}_g)$ was studied. The discriminant of $Q_\tau(\bar{n}_g)$ takes the form $\Delta_Q(\tau) = 1 - 2\tau$, and we know that the critical temperature satisfies $\Delta_Q(\tau_{\text{cp}}) = 0$, giving $\tau_{\text{cp}} = 1/2$. In this case, the roots of $Q_\tau(\bar{n}_g)$, given by

$$n_1(\tau) = \frac{1}{2} - \frac{\sqrt{\Delta_Q(\tau)}}{2}, \quad (47)$$

$$n_2(\tau) = \frac{1}{2} + \frac{\sqrt{\Delta_Q(\tau)}}{2}, \quad (48)$$

coincide and are equal to $n_{\text{cp}} = 1/2$. The last expressions also show that for $\tau > \tau_{\text{cp}}$, $Q_\tau(\bar{n}_g)$ has no real roots and, hence, the second order coefficient c_φ does not vanish. This means that in such a case the condition $b_\varphi(\bar{n}_g, \tau, \eta) = 0$ defines only one state of equilibrium, and, therefore, phase transitions can only occur if $\tau < 1/2$.

We emphasize that, for Thirring's model, the coefficients (42), (43), and (44) of the Landau expansion can be alternatively obtained from the free energy (12), instead of the method we employed here. In fact, from (12), the remaining coefficient of (37) takes the form

$$e_\varphi(\bar{n}_g, \tau, \eta) = \frac{1}{12} \left[\frac{1}{\bar{n}_g^3} + \frac{1}{(1-\bar{n}_g)^3} \right]. \quad (49)$$

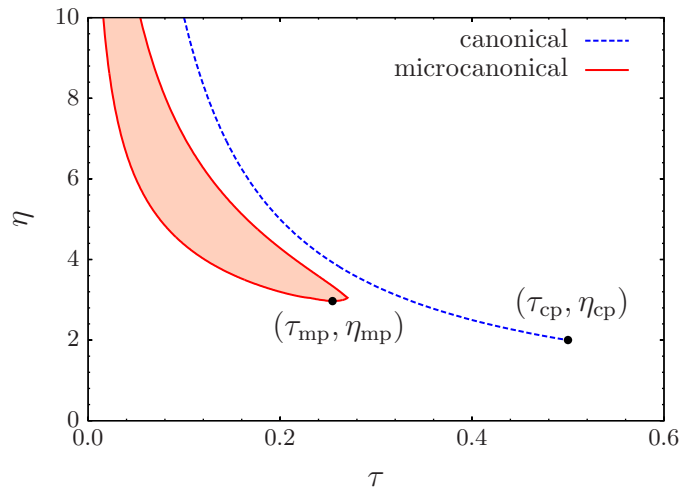


Figure 4. Comparison of the microcanonical and canonical phase diagrams. The reduced volume η is shown as a function of the temperature τ at the transition line of the two ensembles. In the microcanonical ensemble, there are two temperature branches that join at the critical point. The temperatures within the region between these two branches are forbidden in the microcanonical ensemble. In the canonical ensemble, τ is a control parameter and, thus, has no discontinuity at the transition line. The critical parameters are $\tau_{\text{mp}} \simeq 0.2547$, $\eta_{\text{mp}} \simeq 2.969$, $\tau_{\text{cp}} = 1/2$ and $\eta_{\text{cp}} = 2$.

However, taking into account that the expansions (14) and (31) do not depend on the model, some general conclusions can be obtained from this method. From equation (40) one sees that at the canonical critical point, where $c_\varphi = 0$, c_0 is different from zero if $b_1 \neq 0$, implying that the two critical points do not coincide in general, regardless of the model. Of course, for a particular model, the Landau expansion may present a symmetry with respect to the order parameter that enforces the condition $b_1 = 0$ [29]; here we consider that there is no such a symmetry. Furthermore, it is important to stress that, according to the Landau theory, we are assuming analyticity of the free energy at the canonical critical point. Analyticity here can be assumed because the system is nonadditive and for these systems actually there is no phase separation at the transition line. Therefore, this discussion does not apply to short-range interacting systems, since these systems do undergo phase separation at a first-order transition, which, in addition, occurs under the same conditions in the different ensembles.

5. Microcanonical and canonical phase diagrams

In this section we will draw a comparison between the microcanonical and canonical phase diagrams. Since the transition is first-order in both ensembles, the two equilibrium configurations associated to the transition are characterized by a jump in \bar{n}_g and, hence, in the associated thermodynamic properties (those which are not control parameters).

In figure 2, we plotted the microcanonical transition line $\eta(\varepsilon)$. This line indicates the points (ε, η) at which phase transition takes place, i.e., when the entropy reaches the same value at the two maxima. We emphasize that both ε and η are control parameters

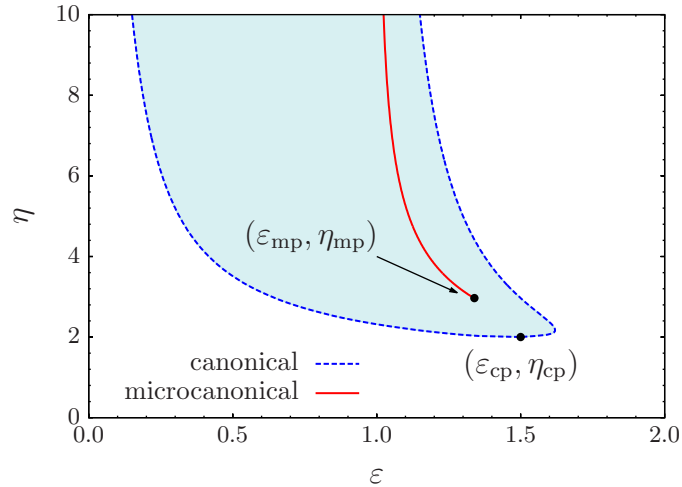


Figure 5. Comparison of the microcanonical and canonical phase diagrams. The reduced volume η is shown as a function of the reduced energy ε at the transition line of the two ensembles. In the canonical ensemble, there are two energy branches that join at the critical point. The energies within the region between these two branches are forbidden in the canonical ensemble. In the microcanonical ensemble, ε is a control parameter and, thus, has no discontinuity at the transition line. The critical parameters are $\varepsilon_{\text{mp}} \simeq 1.339$, $\eta_{\text{mp}} \simeq 2.969$, $\varepsilon_{\text{cp}} = 3/2$ and $\eta_{\text{cp}} = 2$.

in the microcanonical ensemble. In figure 3, we showed the canonical transition line $\eta(\tau)$ containing the points (τ, η) at which a phase transition occurs in the canonical ensemble, corresponding to the coincidence of the two free energy minima. We recall that τ and η are the control parameters in this ensemble.

On the one hand, in the microcanonical case, the jump in \bar{n}_g produces a jump in the temperature. This can be seen in figure 4 in the microcanonical phase diagram in the (τ, η) plane: we plot η at the transition line as a function of the microcanonical temperature τ . The phase diagram has two branches starting at small temperatures and high η that join smoothly at the critical point. According to (8), the microcanonical temperature at the critical point is $\tau_{\text{mp}} \simeq 0.2547$. We highlight that the temperatures between the two branches of the phase diagram are forbidden for the system in the microcanonical ensemble. In addition, for comparison purposes, in figure 4 the canonical phase diagram is also shown, where τ is a control parameter and thus has no discontinuity. We observe that the microcanonical and canonical critical points are far from each other and that the temperatures corresponding to the canonical phase transition are allowed in the microcanonical ensemble.

On the other hand, in the canonical ensemble the jump in \bar{n}_g at the transition produces a jump in the energy, as shown in figure 5 in the phase diagram in the (ε, η) plane. In this diagram, there are two energy branches that join smoothly at the canonical critical point, the energy at this point being $\varepsilon_{\text{cp}} = 3/2$. Moreover, due to the jump, the values of the energy between the two branches are forbidden in the canonical ensemble. We finally observe that the energies at the transition line in the microcanonical ensemble,

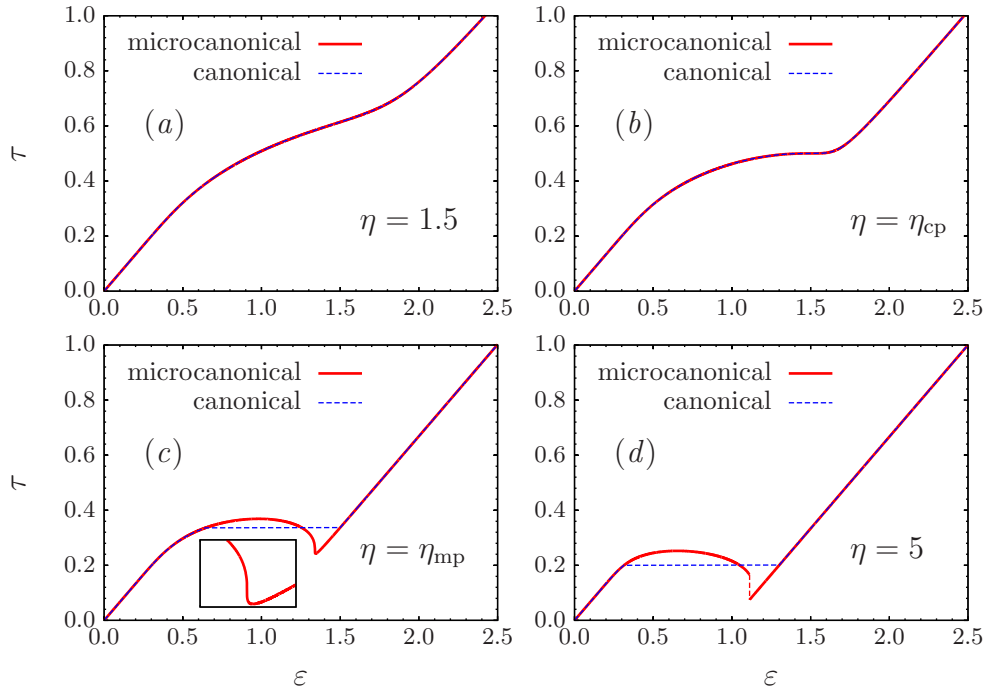


Figure 6. Caloric curves in the microcanonical and canonical ensembles for several values of the reduced volume η . For $\eta \leq \eta_{\text{cp}}$ the two ensembles are equivalent, as shown in (a) and (b). In (c) and (d), a region of nonconcave entropy, containing a region with negative specific heat, in the microcanonical ensemble appears for $\eta > \eta_{\text{cp}}$, which is jumped over by a first order transition in the canonical ensemble. In (c), the curve has a vertical tangent when approaching from both the left and the right to the critical energy ε_{mp} , occurring just before the local minimum (see the enlargement in the inset). For $\eta > \eta_{\text{mp}}$, in (d), the system develops a temperature jump in the microcanonical ensemble. This jump is denoted with a red dashed line.

also shown in figure 5, lie within the region of forbidden canonical energies.

To get a clearer picture of the behavior of the system when the energy is a control parameter, in comparison with the situation in which the system is in contact with a thermostat at fixed temperature, in figure 6 we show several caloric curves in both the microcanonical and canonical ensembles. These curves are shown for different values of the reduced volume η . When $\eta \leq \eta_{\text{cp}}$ the temperature-energy relation $\tau(\varepsilon, \eta)$ is invertible –in the sense that $\varepsilon(\tau, \eta)$ can be unequivocally obtained from it–, and the microcanonical and canonical ensembles are equivalent. Notice that in this case the Legendre-Fenchel transform (9) reduces to the usual Legendre transform. For values of η such that the temperature-energy relation is not invertible in the microcanonical ensemble, the system undergoes a first-order phase transition in the canonical ensemble. Moreover, for $\eta > \eta_{\text{mp}}$, the microcanonical phase transition is always jumped over by the transition in the canonical ensemble. This is, of course, in agreement with the fact that the microcanonical critical point ($\eta = \eta_{\text{mp}}$) lies in the region of forbidden energies in the canonical ensemble.

We emphasize that at the canonical critical point the specific heat diverges in both

the microcanonical and canonical ensembles. This state of the system is described exactly in the same way in the two ensembles. However, while at $\tau = \tau_{\text{cp}}$ and $\eta = \eta_{\text{cp}}$ there is a second-order phase transition in the canonical ensemble (that becomes first-order for $\eta > \eta_{\text{cp}}$ at the corresponding τ), at this point there is no transition in the microcanonical ensemble. To see that the mere presence of a diverging specific heat (or a vanishing derivative of the curve τ vs. ε) is not sufficient to say that there is a phase transition in the microcanonical ensemble, consider for instance the caloric curve for a value of η such that $\eta_{\text{cp}} < \eta < \eta_{\text{mp}}$, which corresponds to a situation between (b) and (c) in figure 6. This curve is continuous with continuous derivative, but with a region of negative specific heat located between the two values of ε at which the curve τ vs. ε has zero derivative. The system does not undergo qualitative changes when passing through any of the points of this curve, which can be achieved by slightly modifying the control parameters in the neighborhood of a given point. The canonical critical point is, for the microcanonical ensemble, just the first point where a vanishing value of the derivative of τ as a function of ε appears. In other words, since the microcanonical specific heat can be written as

$$c_{\text{micro}} = - \left(\frac{\partial s}{\partial \varepsilon} \right)^2 \left(\frac{\partial^2 s}{\partial \varepsilon^2} \right)^{-1}, \quad (50)$$

an inflection point in $s(\varepsilon)$ with vanishing second derivative may produce a diverging microcanonical specific heat.

It is interesting to note that the regions of ensemble inequivalence and the occurrence of phase transitions in both ensembles can be deduced from singular points in the $s(\varepsilon, \eta)$ curve or, equivalently, from the microcanonical temperature-energy relation $\tau(\varepsilon, \eta)$. We identify two different codimension 1 singularities, as classified in [26]. Notice that here η is the (only one) parameter, in addition to the energy, that can produce a change in the structure of $s(\varepsilon, \eta)$ or the caloric curve. These singular points can be observed in figure 6, as we discuss in what follows. At $\eta = \eta_{\text{cp}}$, a singularity arises due to convexification, in which a point with horizontal tangent appears in the curve $\tau(\varepsilon, \eta_{\text{cp}})$ (the entropy is concave at this point). This corresponds to the canonical critical point. The second singularity occurs at $\eta = \eta_{\text{mp}}$, which is a maximization singularity, in that a point with vertical tangent appears in the curve $\tau(\varepsilon, \eta_{\text{mp}})$. Such a point correspond to the microcanonical critical point.

6. Conclusions

We have studied the phase diagrams of Thirring's model [8] in both the microcanonical and canonical ensembles. Due to the nonadditive character of the system, these two ensembles are not equivalent and the corresponding phase diagrams are different from each other. Using the Landau theory of phase transitions, as done in [29], the coefficients of the Landau expansion of the canonical free energy can be written in terms of the coefficients of the microcanonical entropy, which permits an analysis of the critical

conditions in which these coefficient vanish. Hence, the critical point at which each first-order transition line terminates can be computed exactly, evincing that they are indeed different. Since the analysis was performed from generic expansions for the entropy and the free energy, it can be inferred that, in general, the critical points in the two ensembles are different. As a difference with respect to [29], here we have considered that there are no symmetries restricting the coefficients of the Landau expansion of the corresponding thermodynamic potentials. Moreover, the comparison of the two phase diagrams shows that the energies at which phase transitions take place in the microcanonical ensemble are not allowed in the canonical ensemble. Conversely, the temperatures at which the transitions take place in the canonical ensemble are accessible to the microcanonical equilibrium configurations.

Furthermore, in this case, the microcanonical entropy and the canonical free energy can be written as a maximization and minimization problem, respectively, with respect to a variable n_g (here representing the fraction of free particles), and the expansion parameter in the Landau expressions can be written as $m = n_g - \bar{n}_g$, where \bar{n}_g is a reference value. In addition, the Landau expansions are complete, at least to the fourth order, and the second order coefficient in the two ensembles is a rational function of the form $f_\lambda(\bar{n}_g)/g_\lambda(\bar{n}_g)$, where $f_\lambda(\bar{n}_g)$ and $g_\lambda(\bar{n}_g)$ are polynomials of the variable \bar{n}_g that depend on the parameter λ . The parameter λ is the energy in the microcanonical case and the temperature in the canonical one. Thus, we have shown that, in general, when this conditions are met, the critical point in each ensemble can be obtained by studying the zeros of the discriminants $\Delta_f(\lambda)$ associated to the polynomials $f_\lambda(\bar{n}_g)$.

Acknowledgments

We thank O Cohen and D Mukamel for fruitful discussions. I L acknowledges financial support through an FPI scholarship (Grant No. BES-2012-054782) from the Spanish Government. This work was partially supported by the Spanish Government under Grant No. FIS2011-22603. We also thank the Galileo Galilei Institute for Theoretical Physics for the hospitality and the INFN for partial support during the completion of this work.

References

- [1] Campa A, Dauxois T, Fanelli D and Ruffo S 2014 *Physics of Long-Range Interacting Systems* (Oxford: Oxford University Press)
- [2] Campa A, Dauxois T and Ruffo S 2009 Phys. Rep. **480** 57
- [3] Bouchet F, Gupta S and Mukamel D 2010 Physica A **389** 4389
- [4] Levin Y, Pakter R, Rizzato F B, Teles T N and Benetti F P C 2014 Phys. Rep. **535** 1
- [5] Antonov V A 1962 Vest. Leningr. Gos. Univ. **7** 135; translation: IAU Symposia 1985 **113** 525
- [6] Lynden-Bell D and Wood R 1968 Mon. Not. R. Astr. Soc. **138** 495
- [7] Lynden-Bell D 1999 Physica A **263** 293
- [8] Thirring W 1970 Zeitschrift für Physik **235** 339
- [9] Padmanabhan T 1990 Phys. Rep. **188** 285

- [10] Chavanis P-H 2002 *Astron. Astrophys.* **381** 340
- [11] Chavanis P-H 2006 *Int. J. Mod. Phys. B* **20** 3113
- [12] de Vega H and Sánchez N 2002 *Nucl. Phys. B* **625** 409
- [13] de Vega H and Sánchez N 2002 *Nucl. Phys. B* **625** 460
- [14] Kiessling M K H and Neukirch T 2003 *Proc. Natl. Acad. Sci.* **100** 1510
- [15] Nicholson D R 1992 *Introduction to Plasma Physics* (Malabar, FL: Krieger)
- [16] Chavanis P-H and Sommeria J 2002 *Phys. Rev. E* **65** 026302
- [17] Bouchet F and Venaille A 2012 *Phys. Rep.* **515** 227
- [18] Miller J 1990 *Phys. Rev. Lett.* **65** 2137
- [19] Onsager L 1949 *Nuovo Cimento Suppl.* **6** 279
- [20] Robert R and Sommeria J 1991 *J. Fluid. Mech.* **229** 291
- [21] Mori T 2010 *Phys. Rev. E* **82** 060103(R)
- [22] Mori T 2011 *Phys. Rev. E* **84** 031128
- [23] Latella I, Pérez-Madrid A, Campa A, Casetti L and Ruffo S 2015 *Phys. Rev. Lett.* **114** 230601
- [24] Ellis R S, Haven K and Turkington B 2000 *J. Stat. Phys.* **101** 999
- [25] Barré J, Mukamel D and Ruffo S 2001 *Phys. Rev. Lett.* **87** 030601
- [26] Bouchet F and Barré J 2005 *J. Stat. Phys.* **118** 1073
- [27] Latella I and Pérez-Madrid A 2013 *Phys. Rev. E* **88** 042135
- [28] Landau L D and Lifshitz E M 1980 *Statistical Physics* Vol. 5 3rd ed. (Oxford: Butterworth-Heinemann)
- [29] Cohen O and Mukamel D 2012 *J. Stat. Mech.* P12017
- [30] Lederhendler A and Mukamel D 2010 *Phys. Rev. Lett.* **105** 150602
- [31] Lederhendler A, Cohen O and Mukamel D 2010 *J. Stat. Mech.* P11016
- [32] Casetti L and Nardini C 2010 *J. Stat. Mech.* P05006
- [33] Casetti L, in preparation